Interconversion of the CD and EF Sites in Oncomodulin. Influence on the Eu^{3+} $^7F_0 \rightarrow {}^5D_0$ Excitation Spectrum†

John F. Kauffman,‡ Raymond C. Hapak,§ and Michael T. Henzl*,§

Departments of Biochemistry and Chemistry, University of Missouri, Columbia, Missouri 65211

Received June 24, 1994; Revised Manuscript Received November 15, 1994⊗

ABSTRACT: The appearance of the parvalbumin Eu^{3+} $^7F_0 \rightarrow {}^5D_0$ spectrum is markedly pH dependent, the result of a hitherto unidentified deprotonation event in the CD ion-binding domain [Treviño, C. L., *et al.* (1991) *J. Biol. Chem. 265*, 9694−9700]. We are studying this phenomenon in the mammalian placental parvalbumin called oncomodulin. As in other parvalbumins, the liganding residues in the CD and EF sites of oncomodulin differ at the $+z$ and $-x$ coordination positions: serine and aspartate, respectively, in the CD site; aspartate and glycine in the EF site. We have prepared a series of oncomodulin variants in which the $+z$ and/or $-x$ residue(s) from one site have been replaced by the corresponding residue(s) from the other. We herein characterize the resulting proteins by Eu^{3+} luminescence spectroscopy. Simultaneous replacement of serine-55 by aspartate and aspartate-59 by glycine affords the CD site with a coordination sphere superficially equivalent to that of the EF site. As observed previously for the S55D mutation [Henzl, M. T., *et al.* (1992) *FEBS Lett. 314*, 130−134], the Eu^{3+} $^7F_0 \rightarrow {}^5D_0$ spectrum of the 55/59 variant is pH independent. Interestingly, replacement of aspartate-94 by serine at the $+z$ position of the EF site of 55/59 imparts pH dependent behavior to the EF site. The identical mutation in the wild-type background likewise imparts pH dependence to the EF site, affording a protein in which both sites display broad signals near 578.2 nm at pH 8. Significantly, a variant in which threonine replaces serine-55 retains the pH dependent spectroscopic signature. These results indicate that the presence of a hydroxyl group at the $+z$ position is sufficient to confer pH dependence on the $^7F_0 \rightarrow {}^5D_0$ spectrum of a parvalbumin EF-hand domain. Importantly, the data also suggest that the component peaks of the low-pH doublet are not site-specific signals, as previously believed. Rather, they probably represent differences in coordination environment arising from differential hydration or conformational heterogeneity. In wild-type oncomodulin, the CD site signal dominates the low-pH spectrum. Since this dominance persists even when serine-55 and aspartate-59 are replaced by the corresponding EF site residues, it appears that the context of the CD binding site, as dictated by the global polypeptide fold, exerts a major influence on the metal ion-binding properties of the site.

Members of the calmodulin superfamily are distinguished by their characteristic Ca^{2+}-binding domain, which comprises a central ion-binding loop flanked by short α-helices (Kretsinger, 1980, 1987; Strynadka & James, 1989). This helix−loop−helix structure is called the "EF-hand" domain or the "calmodulin fold". The parvalbumins, a subset of the calmodulin superfamily, contain two functional EF-hand domains (Wnuk *et al.*, 1982). These vertebrate-specific proteins are abundant in specific skeletal myofibrils, select neuronal subpopulations, and certain endocrine cells (Heizmann & Berchtold, 1987). They are believed to function as cytosolic Ca^{2+} buffers in these tissue settings (Heizmann *et al.*, 1989). The two Ca^{2+}-binding domains are known as the CD[1] and EF sites, a reference to the helical elements that flank the ion-binding loops. In fact, it was the X-ray crystallographic structure of the carp parvalbumin EF domain that established the "EF-hand" structural paradigm (Kretsinger & Nockolds, 1973). Although the parvalbumin CD and EF sites are generally indistinguishable in Ca^{2+} titrations, displaying dissociation constants between 2−10 nM, work by Sykes and co-workers (Williams *et al.*, 1984) indicates that the CD site is substantially more rigid than the EF site. Whether this behavior is dictated by the folding of the polypeptide chain or the immediate coordination environment, or some combination thereof, is not presently known.

Oncomodulin is the oncofetal parvalbumin discovered by MacManus (1979). Although normal expression of oncomodulin is confined to the fetal placenta (Brewer & MacManus, 1987), the protein frequently reappears upon neoplastic transformation and is detectable in approximately 80% of all mammalian tumors (Gillen *et al.*, 1988). Relative to other parvalbumins, the CD and EF sites display substantially lower affinity for Ca^{2+} and are decidedly inequivalent. The apparent dissociation constants for Ca^{2+} are approximately

† This work was supported by NSF Award MCB92-96171 (to M.T.H.).

‡ Department of Chemistry.

§ Department of Biochemistry.

⊗ Abstract published in *Advance ACS Abstracts,* January 1, 1995.

[1] Abbreviations: MES, 2-(*N*-morpholino)ethanesulfonic acid; HEPES, 4-(2-hydroxyethyl)-1-piperazineethanesulfonic acid; EDTA, ethylenediaminetetraacetic acid; CD site, the metal ion-binding site in the parvalbumins flanked by the C and D helical segments; EF site, the parvalbumin metal ion-binding site flanked by the E and F helical segments. Single-site mutations are denoted by bracketing the site of mutation with the one-letter abbreviation for the original and substituted amino acid residues, respectively. Multiple-site mutations are denoted by listing the sites of mutation separated by slashes, and it is understood that we are replacing the CD-site residue with the corresponding EF-site residue or vice versa.

0006-2960/95/0434-991$09.00/0

0.04 and 0.8 μM, respectively, for the CD and EF sites (Hapak *et al.*, 1989; Cox *et al.*, 1990). The characteristic rigidity of the CD site observed in other parvalbumins is even more appararent in oncomodulin (Williams *et al.*, 1987).

One manifestation of the increased rigidity of the parvalbumin CD domain is a strong preference for the larger lanthanide ions at the beginning of the series. The potential utility of the lanthanide ions as probes of Ca^{2+}-binding systems has been recognized for more than 20 years [for reviews, see Horrocks and Sudnick (1981), Martin, (1983), and Evans, (1990)]. They share with Ca^{2+} a similar preference for oxygen ligands and high coordination numbers and, especially those ions in the middle of the series, are comparable in size to Ca^{2+}. Owing to the presence of 4f valence electrons, they undergo accessible transitions in the UV−visible region of the electromagnetic spectrum, making them amenable to spectroscopic analysis.

Eu^{3+} absorbs weakly near 580 nm, the result of a transition between the $^7F_0$ ground state and the $^5D_0$ excited state (Samelson *et al.*, 1966). Since the total angular momentum is unchanged by this electronic rearrangement, the $^7F_0 \rightarrow {}^5D_0$ transition is strongly forbidden. The absorption is too weak to observe directly in typical solutions of biological macromolecules ($\epsilon \approx 0.01$ M^{-1} cm^{-1}). Instead, one obtains the corresponding excitation spectrum, exciting the ion with a tunable laser between 575 and 582 nm and monitoring the subsequent emission (usually at 615 nm) that accompanies return of the ion to the ground-state manifold.

The $^7F_0 \rightarrow {}^5D_0$ transition is a potentially useful investigative tool (McNemar & Horrocks, 1990). Both ground- and excited electronic states are nondegenerate ($J = 0$) and, therefore, cannot be split into sublevels by the surrounding ligand field. As a consequence, each distinct Eu^{3+} species in a sample should yield a single peak in the $^7F_0 \rightarrow {}^5D_0$ spectrum, simplifying data interpretation. Thus, the original observation (Horrocks & Collier, 1981; Rhee *et al.*, 1981) of three spectral features in the Eu^{3+} $^7F_0 \rightarrow {}^5D_0$ spectrum of carp parvalbumin at pH 7.5 was puzzling and led to the suggestion that these proteins contain three binding sites for lanthanide ions. In fact, they contain just two, and the extra peak in the Eu^{3+} spectrum arises from a pH dependent spectroscopic alteration (Henzl *et al.*, 1985).

At low pH (pH 5), parvalbumin preparations containing two molar equivalents of Eu^{3+} exhibit a partially resolved doublet centered near 579.5 nm. At higher pH values, the signal arising from the CD site is replaced by a broad, intense signal having a maximum between 578.1 and 578.4 nm. The pK_a for this transition is generally between 8.0 and 8.5. Oncomodulin behaves similarly, except that the pK_a for the alteration is lower (Henzl *et al.*, 1986; Henzl & Birnbaum, 1988). Recently, we showed that replacement of serine-55 in oncomodulin by aspartate abolishes the pH dependent spectral alteration (Henzl *et al.*, 1992), suggesting that deprotonation of the serine hydroxyl, an invariant feature of the parvalbumin CD site, is responsible for the phenomenon.

This finding led us to ask whether the hydroxyl group at the $+z$ ligand position was sufficient to confer pH dependence on an EF-hand site. Thus, we have prepared and characterized a series of oncomodulin variants in which the ligand arrays in the CD and EF sites have been interconverted. The sequence of preparation was wild-type →S55D →55/59→ 55/59/94 → 55/59/94/98. In essence, our strategy was to convert the CD site into a "quasi-EF" site and vice versa, finally ending with a protein in which the sites were reversed. We have also examined each of the individual mutations, as well as the double variants 55/59 and 94/98. In this paper, all of the variant proteins are characterized in terms of their Eu^{3+} luminescence properties. Their Ca^{2+}-binding properties will be described elsewhere (R.C.H. and M.T.H., manuscript in preparation).

MATERIALS AND METHODS

$EuCl_3$ and $TbCl_3$ were purchased from Aldrich Chemical Co. All other chemicals were reagent grade and were obtained either from Sigma Chemical Co. or Fisher Scientific Co.

The prokaryotic expression system for oncomodulin employed in this work is described in Hapak and Henzl (1994). Mutations were introduced into the oncomodulin coding system via oligonucleotide-directed mutagenesis of a double-stranded template, employing the Clontech Transformer kit. Each of the mutations was confirmed by DNA sequencing, employing Sequenase (United States Biochemical Co., Inc.).

The recombinant oncomodulin variants, expressed at roughly 20 mg/g of cell paste, were purified as previously described (Hapak *et al.*, 1989). Prior to analysis, residual divalent cations were removed from the protein preparations by passage over EDTA-derivatized agarose (Haner *et al.*, 1984). Protein concentrations were determined by titration with Tb^{3+}, monitoring the marked increase in Tb^{3+} luminescence that accompanies binding of the lanthanide to the protein. The endpoint of the titration, signaled by a plateau in emission intensity, corresponds to the addition of two molar equivalents of Tb^{3+}. Solutions of Tb^{3+} and Eu^{3+} were standardized by titration with EDTA, employing xylenol orange as an indicator (Lyle & Rahman, 1963). The samples (100 μM) contained 0.15 M NaCl, 0.015 M MES, and 0.015 M HEPES. They were adjusted to pH 5.0 and pH 8.0 with 1 M HCl and NaOH, respectively. Two equivalents of Eu^{3+} were added just prior to acquiring the spectrum. This precaution was taken to minimize slow precipitation of the lanthanide ion at the higher pH value.

Equilibrium dialysis was performed in Lucite dialysis blocks of standard design. Lateral transfer of material between wells was prevented by the use of hand-cut Parafilm gaskets and by the use of four stainless steel fasteners per well. The dialysis blocks and Parafilm gaskets were soaked in 3% HNO_3 and throughly rinsed with deionized water prior to assembly. The dialysis membrane was prepared from Spectrapor 1 tubing (molecular weight cut-off 6000−8000) that had been washed in hot (70 °C) 1% sodium carbonate, thoroughly rinsed in deionized water, and stored in 20% ethanol. Immediately prior to use, the tubing was cut along one edge, opened flat, and then soaked for 30 min in 3% HNO_3, after which it was thoroughly rinsed in Nanopure water until the pH of the rinse solution approached 7.

Samples (0.60 mL) of the variant proteins were introduced via syringe into the chambers on one side of the dialysis membrane, and 0.60 mL aliquots of buffer were placed in the opposing chambers. Each protein sample contained 120 nmol of protein (200 μM) and 216 nmol of Eu^{3+} (360 μM, 1.8 molar equivalents). The buffer solution consisted of 0.15 M NaCl, 0.015 M MES-NaOH, and 0.015 M HEPES-NaOH, pH 6.0. After the samples were in place, the dialysis blocks

were allowed to equilibrate for 20 h at room temperature with continuous agitation. Following equilibration, the buffer samples were analyzed for Eu^{3+} by adding EDTA and comparing the intensity of the Eu^{3+} $^7F_0 \rightarrow {}^5D_0$ spectrum to Eu-EDTA standards of known concentration. The detection limit for Eu-EDTA was 0.3 μM.

Eu^{3+} $^7F_0 \rightarrow {}^5D_0$ excitation spectra were acquired between 576.0 and 581.0 nm. A rhodamine 6G dye laser, synchronously pumped by the 532 nm output of a mode-locked Nd:YAG laser, served as the excitation source. Average output was 150 mW. A three-plate birefringent filter with a bandwidth of 0.05 nm was employed as the wavelength selector. The excitation wavelength was scanned in 0.05 nm increments with a stepper motor, reduction gears, and a timing belt. The stepper motor was controlled by a desktop computer via the digital output of an ADC board (Data Translation Inc., model DT2812). The signals at 579.60 and 580.12 nm from a 100 μM solution of Eu-EDTA were employed for wavelength calibration (Albin & Horrocks, 1985). Fluorescence at 614 nm was collected at 90° to the plane of excitation with f/1 optics and was focused into a 0.25 m monochromator, after passage through a 620 nm bandpass filter. Fluorescence intensity was measured with a photomultiplier tube operating in photon-counting mode. The output was sent through a discriminator and pulse-shaping electronics and then to the clock input of the counter on the ADC board. Fluorescence counts were collected at each wavelength for a fixed dwell time (typically 1 s), and a single scan consisted of 100 data points. Typically, 10 scans were acquired to average out fluctuations in source intensity.

Deconvolution of the resulting spectra was performed with PeakFit (Jandel Scientific Co.). The Voight function, a convolution of Gaussian and Lorentzian functions, was employed for the modeling. It is capable of fitting the wings of the $^7F_0 \rightarrow {}^5D_0$ spectra more accurately than either a Gaussian or Lorentzian function alone [e.g., see McNemar and Horrocks (1990)].

RESULTS AND DISCUSSION

This paper is concerned with changes in the Eu^{3+} luminescence spectrum of oncomodulin, and other parvalbumins by extension, resulting from mutations which interconvert the ligand arrays in the CD and EF sites. The data lead us to several important conclusions. Foremost, the pH dependence of the parvalbumin $^7F_0 \rightarrow {}^5D_0$ spectrum results from deprotonation of a coordinated serine hydroxyl group. Secondly, the components of the partially resolved doublet observed near 579.5 nm at low pH probably correspond to distinct hydration states of the bound ions, or to distinct protein conformations, rather than to the individual binding sites, as previously believed. Thirdly, although the identities and ionization states of the liganding groups modulate the spectroscopic parameters of the CD and EF sites, it is apparent that the geometry of the site imposed by the folded polypeptide exerts a controlling influence on the spectroscopic intensity. Finally, we see evidence for a conformational interaction, or cooperativity, between the CD and EF sites.

In the following paragraphs, we address each of these topics in turn. The Eu^{3+} spectral parameters for all of the variants that we have examined are summarized in Table 1, and schematic diagrams of their corresponding ligand arrays are displayed in Figure 1 for ready comparison. As discussed below, the observed spectra are not simple two-component spectra but result instead from the superposition of at least four signals. For this reason, the parameters listed in Table 1 should be regarded as apparent values.

Estimates of Eu^{3+} Binding Affinities. Our analysis of the spectroscopic data presented below assumes that all of the Eu^{3+} added to the protein samples is bound. To test this assumption, we dialyzed samples containing 200 μM protein and 360 μM Eu^{3+} against an equal volume of buffer. After equilibration, the buffer samples were then analyzed for Eu^{3+}. The concentrations thereby determined were used to estimate dissociation constants for the weaker sites, K_{Eu}, employing the following expression:

$$K_{Eu} = \frac{[P][Eu^{3+}]}{[Eu{\cdot}P]}$$

where [P] is the concentration of the unoccupied weaker site, $[Eu^{3+}]$ is the free Eu^{3+} concentration, and [Eu·P] is the concentration of the weaker binding site occupied by Eu^{3+}. Since the total protein concentration was 200 μM and since the maximal Eu^{3+} concentration available for binding at the weaker site was 160 μM, [P] was equal to $(40 + [Eu^{3+}])$ and [Eu·P] was equal to $(160 - [Eu^{3+}])$. The calculated K_{Eu} values are listed in Table 2. An upper limit is given in those cases for which the measured $[Eu^{3+}]$ was substantially below the 0.3 μM detection limit.

With the exceptions of D59G and D94S, all of the estimated dissociation constants were 0.12 μM or less. Under the conditions employed for the spectroscopic analyses (100 μM protein, 200 μM total Eu^{3+}), a K_{Eu} = 0.12 μM should yield a free Eu^{3+} concentration of just 3.4 μM. Thus, for the majority of the variants we examined, the assumption of tight binding appears to be warranted. Interestingly, D59G and D94S exhibited the lowest affinities for Eu^{3+}, consistent with their behavior in Ca^{2+}-binding assays (R.C.H. and M.T.H., manuscript in preparation). From the K_{Eu} value determined for D59G (0.25 μM), we calculate that 95% of the weaker site should be occupied under the conditions employed for spectroscopy. The 1.2 μM value determined for D94S translates to 90% occupation of the weaker site. We have not attempted to correct for this incomplete binding. However, it should be borne in mind that the signal intensities listed for D94S may be underestimated by ≈10%.

pH Dependence of the Eu^{3+} $^7F_0 \rightarrow {}^5D_0$ Spectrum. In common with other parvalbumins, the Eu^{3+} $^7F_0 \rightarrow {}^5D_0$ spectrum of oncomodulin is strongly pH-dependent. At pH 5.0, the spectrum of the fully bound protein consists primarily of a single peak centered at 579.4 nm. As shown in Figure 2A, deconvolution places the component peaks at 579.24 and 579.52 nm. We have previously interpreted these peaks as arising from the CD and EF sites, respectively. However, data presented below indicate that the CD signal dominates the spectrum and includes contributions from both spectral features.

The sloping baseline observed in the $^7F_0 \rightarrow {}^5D_0$ spectrum of wild-type oncomodulin at pH 5.0 actually reflects the onset of the pH dependent spectroscopic alteration. As the pH is increased, the spectrum near 579.5 nm is largely replaced by a broad, intense spectrum at higher energy (Figure 2B). Deconvolution indicates that the high-pH spectrum consists

Table 1: Eu^{3+} $^7F_0 \rightarrow {}^5D_0$ Spectral Parameters, at pH 5.0 and 8.0, for Oncomodulin Variants

variant	pH	peak position (nm)	relative amplitude	peak area	apparent line width (nm)	Voight width 1	Voight width 2
wild-type	5.0	577.67 ± 0.97	4.1×10^3	4.4×10^3	0.86	0.33	0.75
		578.28 ± 1.6	1.17×10^4	2.07×10^4	1.44	0.45	1.1
		579.24 ± 0.15	1.25×10^5	9.94×10^4	0.60	0.19	1.10
		579.52 ± 0.07	8.12×10^4	3.20×10^4	0.37	0.22	6.1×10^{-9}
	8.0	577.56 ± 0.22	1.58×10^5	2.40×10^5	1.19	0.25	2.08
		578.14 ± 0.11	2.33×10^5	3.14×10^5	1.07	0.36	1.00
		579.24 ± 0.08	2.94×10^4	1.05×10^4	0.33	0.19	0.06
		579.52 ± 0.05	3.70×10^4	1.08×10^4	0.27	0.16	9.9×10^{-9}
S55D	5.0	579.40 ± 0.04	1.17×10^5	9.58×10^4	0.72	0.38	0.19
		579.68 ± 0.01	6.22×10^4	1.98×10^4	0.30	0.18	3.5×10^{-4}
	8.0	579.40 ± 0.05	1.17×10^5	9.87×10^4	0.73	0.38	0.22
		579.70 ± 0.01	9.30×10^4	2.95×10^4	0.30	0.18	6.8×10^{-9}
S55T	5.0	578.50 ± 0.24	2.1×10^3	3.0×10^3	1.12	0.25	2.0
		578.81 ± 1.41	2.6×10^3	2.4×10^3	0.72	0.24	1
		579.28 ± 0.05	5.99×10^4	4.32×10^4	0.58	0.24	0.63
		579.66 ± 0.03	8.19×10^4	3.74×10^4	0.43	0.26	2.5×10^{-8}
	8.0	577.55 ± 0.06	1.51×10^5	2.25×10^5	1.21	0.38	1.13
		578.32 ± 0.02	1.97×10^5	2.12×10^5	0.83	0.26	1.13
		579.32 ± 0.42	2.38×10^4	1.21×10^4	0.44	0.23	0.21
		579.63 ± 0.26	2.80×10^4	1.09×10^4	0.37	0.22	2.5×10^{-4}
55/59	5.0	579.38 ± 0.07	1.24×10^5	1.03×10^5	0.72	0.38	0.21
		579.66 ± 0.01	1.19×10^5	4.08×10^4	0.32	0.19	2.6×10^{-9}
	8.0	578.67 ± 1.5	2.33×10^4	5.35×10^5	1.94	0.35	2.51
		579.33 ± 0.06	7.15×10^4	5.43×10^4	0.69	0.38	0.12
		579.71 ± 0.01	1.09×10^5	4.47×10^4	0.38	0.23	2.3×10^{-9}
55/59/94	5.0	579.39 ± 0.02	1.46×10^5	1.08×10^5	0.61	0.28	0.43
		579.71 ± 0.01	2.04×10^5	7.00×10^4	0.32	0.19	7.0×10^{-10}
	8.0	576.97 ± 0.05	3.46×10^4	5.59×10^4	1.40	0.27	2.26
		578.06 ± 0.02	9.45×10^4	1.62×10^5	1.37	0.34	1.59
		579.44 ± 0.03	8.57×10^4	4.80×10^4	0.53	0.32	9.6×10^{-10}
		579.72 ± 0.01	2.04×10^5	7.31×10^4	0.32	0.18	0.11
D94S	5.0	577.10 ± 13	3.1×10^3	7.1×10^3	2.28	0.48	2.1
		578.36 ± 0.82	9.9×10^3	1.48×10^4	1.40	0.84	1.7×10^{-8}
		579.23 ± 0.26	1.03×10^5	7.92×10^4	0.58	0.19	1.04
		579.46 ± 0.17	6.36×10^4	2.86×10^4	0.42	0.25	0.023
	8.0	577.36 ± 0.08	2.11×10^5	3.92×10^5	1.57	0.36	1.82
		578.23 ± 0.02	3.33×10^5	3.67×10^5	1.03	0.62	2.7×10^{-11}
94/98	5.0	576.77 ± 6.1	4.4×10^3	9.3×10^3	2.25	0.52	1.82
		578.15 ± 0.34	1.29×10^4	1.86×10^4	1.35	0.81	1.1×10^{-10}
		579.23 ± 0.31	9.71×10^4	7.81×10^4	0.62	0.21	0.94
		579.47 ± 0.12	6.13×10^4	3.09×10^4	0.42	0.20	0.38
	8.0	577.16 ± 0.05	1.92×10^5	3.28×10^5	1.47	0.39	1.5
		578.16 ± 0.01	4.26×10^4	5.12×10^5	1.10	0.66	2.2×10^{-12}
55/59/94/98	5.0	576.90 ± 1.95	5.6×10^3	1.18×10^4	2.08	0.36	2.59
		578.13 ± 0.24	8.1×10^3	1.14×10^4	1.08	0.29	1.49
		579.30 ± 0.02	9.86×10^4	7.85×10^4	0.62	0.22	0.85
		579.69 ± 0.01	1.58×10^5	6.09×10^4	0.36	0.22	8.0×10^{-10}
	8.0	577.04 ± 0.05	9.65×10^4	1.46×10^5	1.47	0.82	0.11
		578.20 ± 0.02	2.12×10^5	2.72×10^5	1.06	0.44	0.59
		579.43 ± 0.12	3.27×10^4	1.45×10^4	0.41	0.24	0.045
		579.73 ± 0.02	1.50×10^5	5.30×10^4	0.33	0.20	6.6×10^{-7}
D59G	5.0	577.59 ± 0.57	1.10×10^4	1.60×10^4	1.15	0.31	1.44
		578.22 ± 0.38	7.29×10^3	6.80×10^3	0.72	0.26	0.90
		579.46 ± 0.09	1.21×10^5	9.83×10^4	0.63	0.23	0.88
		579.67 ± 0.02	2.00×10^4	5.21×10^3	0.24	0.15	1.2×10^{-9}
	8.0	577.64 ± 0.18	9.27×10^4	1.81×10^5	1.65	0.41	1.62
		578.24 ± 0.04	1.65×10^4	2.67×10^5	1.30	0.43	1.0
		579.45 ± 0.11	3.10×10^4	1.77×10^4	0.51	0.29	0.11
		579.66 ± 0.06	2.60×10^4	7.56×10^3	0.28	0.16	1.9×10^{-9}
G98D	5.0	576.99 ± 0.77	4.3×10^3	6.5×10^3	1.24	0.12	4.9
		578.10 ± 0.14	1.31×10^4	1.70×10^4	1.19	0.67	0.093
		579.24 ± 0.08	7.88×10^4	5.89×10^4	0.57	0.19	1.04
		579.55 ± 0.04	8.14×10^4	3.76×10^4	0.40	0.21	0.22
	8.0	577.14 ± 0.04	5.93×10^4	8.93×10^4	1.21	0.088	6.8
		578.12 ± 0.01	2.51×10^5	3.51×10^5	1.24	0.64	0.24
		579.28 ± 0.04	2.77×10^4	1.56×10^4	0.38	0.04	4.9
		579.53 ± 0.04	1.84×10^4	6.4×10^3	0.44	0.37	0.52

of two components having maxima at 577.56 and 578.14 nm. This behavior is similar to that observed for other members of the parvalbumin family, except that the apparent pK_a for the spectral alteration is substantially lower. Since the pK_a for the spectral alteration is 6.0, it is essentially complete (>99%) at pH 8.0. Thus, the residual spectrum near 579.5 nm at pH 8.0 must correspond to the ion bound at the EF site. Importantly, notice that spectral deconvolution indicates that the EF signal has two components: at 579.24 and 579.52 nm.

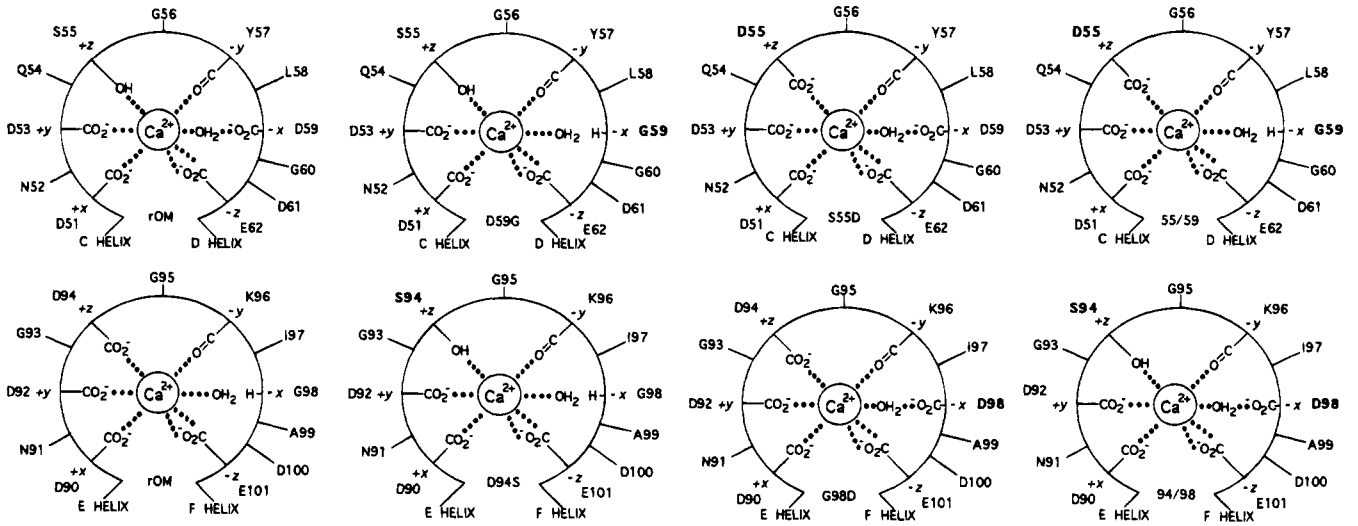

FIGURE 1: Ligand arrays for relevant oncomodulin variants. The pattern of coordination (to Ca^{2+}) within the central binding loop of a helix−loop−helix motif is depicted in the cartoons above. With the exception of the $-y$ ligand, contributed by a peptide carbonyl group, ligands are donated by side-chain oxygen atoms or water. Putative alterations in the CD (top) and EF (bottom) sites resulting from the mutations discussed in the text are displayed together with the wild-type binding sites (far left).

Table 2: Estimated Eu^{3+} Dissociation Constants for Weaker Binding Site in rOM Variant Proteins

rOM Variant	estimated K_{Eu} (μM)[a]	free [Eu^{3+}] during spectroscopic analysis (μM)[b]	fraction of weaker site occupied during spectroscopic analysis[c]
S55D	0.10	3.2	0.97
D59G	0.25	4.9	0.95
D94S	1.2	10.4	0.90
G98D	0.12	3.4	0.97
S55T	0.10	3.2	0.97
55/59	<0.075	<2.7	>0.97
94/98	0.075	2.7	0.97
55/59/94	<0.075	<2.7	>0.97
55/59/94/98	0.10	3.2	0.97

[a] Measured by single-point equilibrium dialysis at pH 6.0, as described in Materials and Methods. [b] Calculation based on estimated K_{Eu} and total protein and Eu^{3+} concentrations of 100 and 200 μM, respectively. [c] Equal to (100 − [Eu^{3+}])/100.

The presence of two components in the high-pH spectrum and the reduction in intensity of both low-pH spectral components originally led to the suggestion that the pH dependent behavior was common to both parvalbumin ion-binding sites (Henzl *et al.*, 1985; Henzl & Birnbaum, 1987; McNemar & Horrocks, 1990). However, subsequent studies with oncomodulin site-specific variants indicated that the phenomenon was restricted to the CD site (Treviño *et al.*, 1991). The ligands in the CD and EF sites differ only at the $+z$ and $-x$ coordination positions, and recent work strongly implicated the $+z$ position in the pH dependent spectral transition. Specifically, replacement of serine-55 in the CD domain with aspartate (S55D) eliminated the pH dependence (Henzl *et al.*, 1992). The $^7F_0 \rightarrow {}^5D_0$ spectra for the fully bound S55D variant at pH 5.0 and 8.0 are displayed in Figure 2 panels C and D, respectively. The absence of the broad peak at 578.1 Å at pH 8.0 suggests that the hydroxyl group of serine-55 is required for the pH-dependent phenotype.

Curious to see whether threonine could substitute for serine in this capacity, we prepared the S55T variant, in which threonine replaces serine-55. The $^7F_0 \rightarrow {}^5D_0$ spectra for the fully bound protein are displayed in Figure 2, panels E (pH 5.0) and F (pH 8.0). Although the intensities of the component peaks in the spectrum at pH 8.0 differ somewhat from those observed for the wild-type protein, it is apparent that S55T retains the pH dependent behavior. Once again, accurate modeling of the residual signal from the EF site near 579.5 requires inclusion of two spectral components for the EF site contribution to the spectrum.

The results obtained with S55D and S55T indicate that the presence of a hydroxyl group at the $+z$ coordination position is required for the pH dependent spectroscopic alteration but not whether it is sufficient. We wondered whether it would be possible to introduce pH dependence into the Eu^{3+} $^7F_0 \rightarrow {}^5D_0$ signal arising from the EF site by simply inserting a hydroxyl group at the $+z$ ligand position. To explore this question, we prepared these additional site-specific oncomodulin variants: 55/59, 55/59/94, D94S, 94/98, and 55/59/94/98. All of these mutations were made at the $+z$ and/or $-x$ positions of the CD and EF binding sites and, in every case, reflect replacement of the CD site residue with the corresponding EF site residue or vice versa. All of the variant proteins retain the capacity to bind two equivalents of lanthanide ion with high affinity.

Concomitant replacement of serine-55 by aspartate and aspartate-59 by glycine, to yield 55/59, endows the CD site with a ligand array identical to the EF site. We refer to this EF-like CD site as a "quasi-EF site". Like S55D, the 55/59 variant displays essentially pH independent spectroscopic behavior. The $^7F_0 \rightarrow {}^5D_0$ spectra obtained at pH 5.0 and 8.0 with a sample of 55/59 containing 2 equiv of Eu^{3+} ion are displayed in Figure 2 panels, G and H, respectively. The reduced intensity of both spectral components at pH 8.0, as well as the broad intensity centered at 578.67 nm, are believed to arise from effective competition of hydroxide ion with the quasi-EF site.

Normally, aspartate-94 occupies the $+z$ coordination site in the EF binding loop. To determine whether the presence of a serine residue at this position is sufficient to confer pH dependence on the Eu^{3+} $^7F_0 \rightarrow {}^5D_0$ signal, we replaced aspartate-94 in the 55/59 variant by serine, yielding 55/59/94. The $^7F_0 \rightarrow {}^5D_0$ spectra at pH 5.0 and 8.0 for fully bound 55/59/94

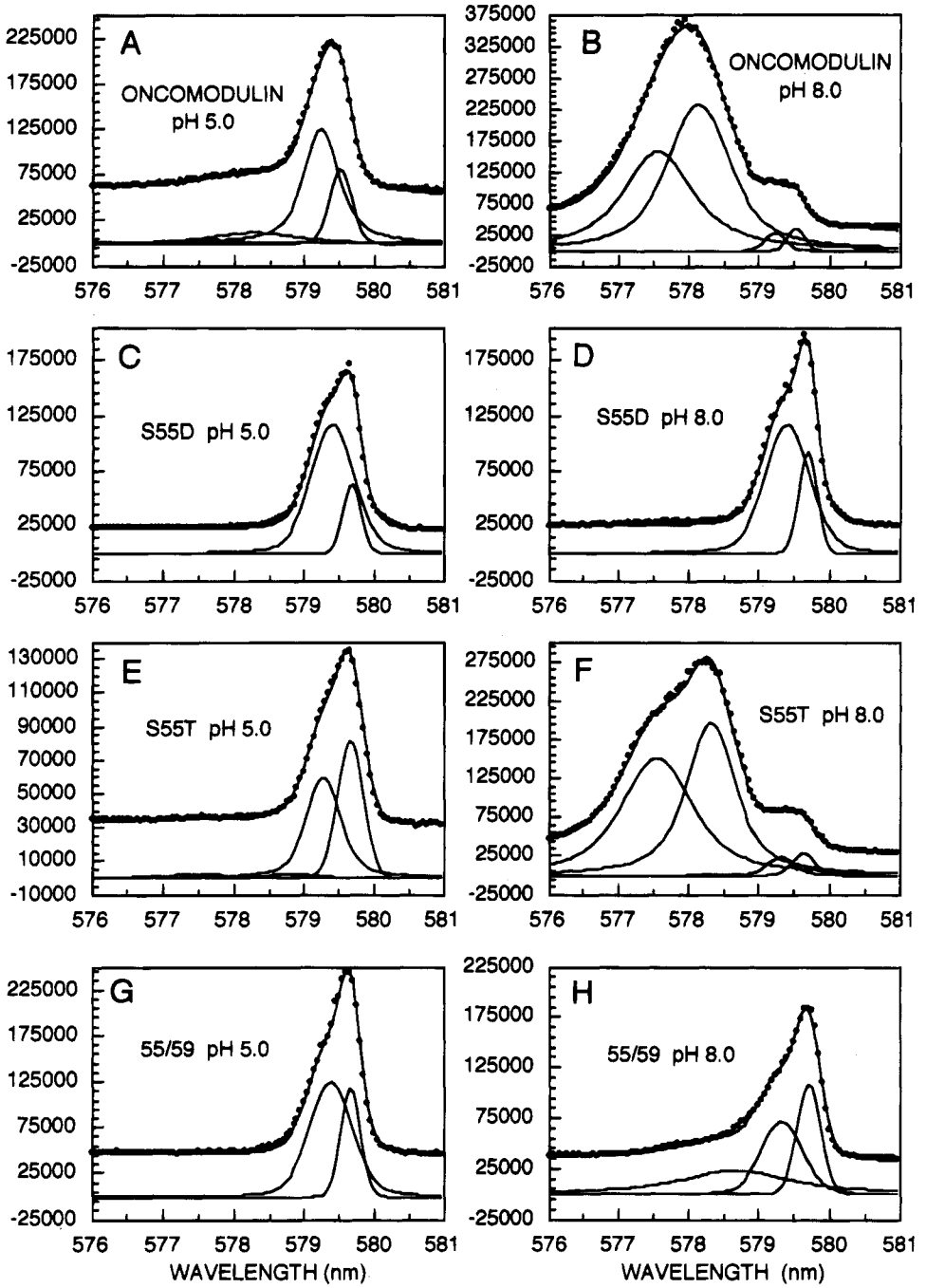

FIGURE 2: Eu^{3+} $^7F_0 \rightarrow {}^5D_0$ excitation spectra of wild-type rOM, S55D, S55T, and 55/59. Spectra were acquired on 100 μM samples of each of these proteins, at pH 5.0 and 8.0, as described in Materials and Methods. The solid line represents the best fit to the data. The component peaks are indicated beneath the spectrum. Apparent spectral parameters are listed in Table 1. For clarity, the baseline has been omitted.

are displayed in Figure 3A, B. Significantly, the 55/59/94 variant has regained the pH dependent spectroscopic phenotype. In contrast to the wild-type protein, however, it is now the EF site of 55/59/94 that has the pH dependent spectroscopic signature. This result indicates that the presence of a hydroxyl group at the $+z$ coordination position can be sufficient to confer pH dependence on the $^7F_0 \rightarrow {}^5D_0$ spectra of EF-hand sites.

The D94S mutation has similar consequences when introduced into the wild-type background (to afford D94S) or into G98D (to afford 94/98). In these variants, however, both binding sites are pH dependent (Figure 3 C−F). This conclusion is supported by (1) the absence of residual intensity near 579.5 nm at pH 8.0, (2) the substantially greater intensities, relative to the wild-type protein, of the D94S and 94/98 high-pH spectra, and (3) the substantially larger apparent line widths of the high-pH signals. Parenthetically, the absence of a residual signal near 579.5 nm indicates that the spectroscopic alterations for both sites are complete at pH 8.0.

Combination of the S55D and D59G mutations furnishes the CD site with an EF-site like coordination sphere. Conversely, the combined D94S and G98D mutations furnish the EF site with a CD-site like coordination sphere. In terms of the liganding groups, the binding sites are reversed in the quadruple variant denoted 55/59/94/98. The $^7F_0 \rightarrow {}^5D_0$ spectra of the quadruple variant 55/59/94/98 are displayed at pH 5 and 8 in Figure 3G, H.

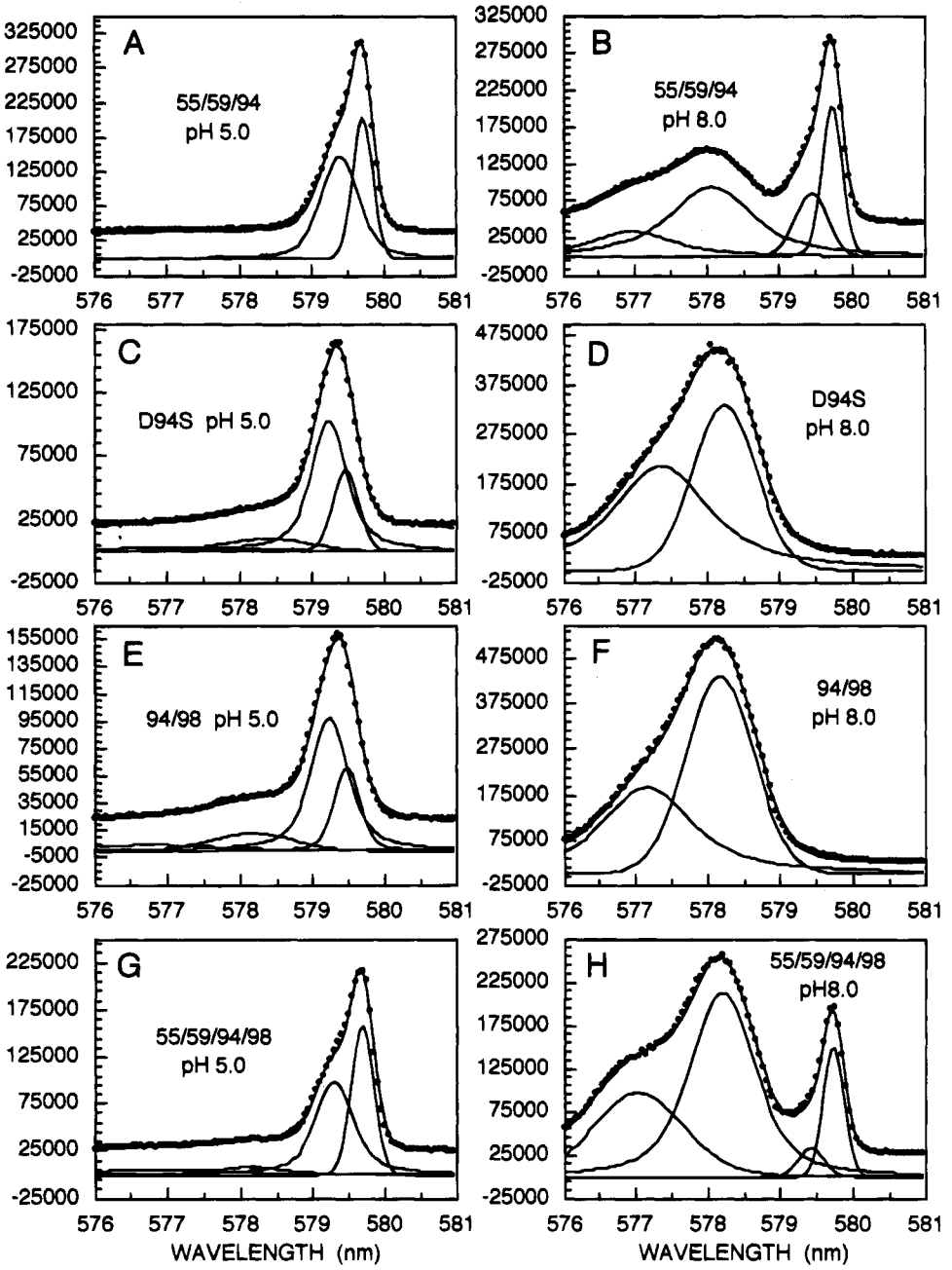

FIGURE 3: Eu^{3+} $^7F_0 \rightarrow {}^5D_0$ excitation spectra of 55/59/94, D94S, 94/98, and 55/59/94/98. Conditions are as described in legend to Figure 2.

It is instructive to compare the residual intensities near 579.5 nm in the high-pH spectra of 55/59/94 or 55/59/94/98 with that of wild-type rOM (or the G98D, D59G, or S55T single-site variants). The residual intensity near that wavelength in the wild-type spectrum reflects the contribution of the EF site. In 55/59/94 and 55/59/94/98, however, it reflects the contribution of the quasi-EF site resulting from the EF→CD mutations in the CD binding loop. Clearly, the signal from the quasi-EF site has a significantly greater area, a point that is discussed in greater detail below.

Reinterpretation of the Low-pH Parvalbumin Spectrum. Since the ground and excited states of the $^7F_0 \rightarrow {}^5D_0$ transition are nondegenerate, *a priori* we expect a one-to-one correspondence between the number of peaks and the number of Eu^{3+} binding sites. Thus, we anticipate that the spectrum of a fully bound parvalbumin will display two signals. The spectrum observed at low pH, consisting of a partially resolved doublet, is in accordance with expectation. It has long been assumed that the higher energy component of the doublet arises from the ion bound at the CD site and that the lower energy component arises from the ion bound at the EF site. However, the luminescence spectra that we obtain from the oncomodulin CD↔EF variants are not consistent with this model. In the subsequent paragraphs, we propose that the low-pH parvalbumin (or oncomodulin) spectrum is dominated by the contribution from the CD site and that, in fact, both components of the partially resolved doublet contribute to the CD site signal. According to this model, the EF signal, which likewise appears to have two components, makes a minor contribution to the overall spectrum in the wild-type protein.

The original assignment of the peaks in the low-pH doublet was made by Horrocks and co-workers (Rhee *et al.*, 1981). Sowadski *et al.* (1978) had shown that crystals of carp parvalbumin could be prepared having Tb^{3+} present only at the EF site. On the basis of luminescence studies with

Table 3: Analysis of Relative CD and EF Site Signal Intensities

variant	pH	peak area at 579.5 nm	combined CD + EF intensities	EF site intensity	CD site intensity	relative areas of CD and EF signals
wild-type	5.0	13.1×10^4 (CD+EF)				
	8.0	2.1×10^4 (EF)	13.1×10^4	2.1×10^4	11×10^4	5.2
S55T	5.0	8.06×10^4 (CD+EF)				
	8.0	2.3×10^4 (EF)	8.06×10^4	2.3×10^4	5.7×10^4	2.5
D59G	5.0	10.3×10^4 (CD+EF)				
	8.0	2.53×10^4 (EF)	10.3×10^4	2.5×10^4	6.8×10^4	2.7
G98D	5.0	9.7×10^4 (CD+EF)				
	8.0	2.2×10^4 (EF)	9.7×10^4	2.2×10^4	7.2×10^4	3.3
55/59/94	5.0	17.1×10^4 (CD+EF)				
	8.0	12.1×10^4 (CD)	17.1×10^4	5.0×10^4	12.1×10^4	2.4
55/59/94/98	5.0	13.9×10^4 (CD+EF)				
	8.0	6.8×10^4 (CD)	13.9×10^4	7.1×10^4	6.8×10^4	1.0

comparable parvalbumin crystals prepared with Eu^{3+}, Rhee *et al.* concluded that the higher wavelength component of the doublet arose from the EF site. When Henzl *et al.* (1985) discussed the lanthanide-binding and luminescence properties of pike parvalbumin III (pI 5.0), they followed the lead of Horrocks, assigning the signal at 579.2 nm to the CD site and the 579.6 nm signal to the EF site. This assignment seemed reasonable, since the higher wavelength component grew in slightly more rapidly during the early stages of a Eu^{3+} titration [Henzl *et al.* (1985), Figure 7]. This interpretation was retained in subsequent papers from both the Horrocks and Henzl laboratories.

In retrospect, there were inconsistencies with this model. For example, as the pH is raised, both components of the low pH spectrum were observed to decrease in intensity. Moreover, they seemed to decrease in parallel. For example, the low- and high-pH spectra of pike and rat parvalbumins, and oncomodulin as well, exhibited apparent isosbestic points. And in the case of rat parvalbumin, spectral deconvolution indicated that the rate of decline was approximately equal for both low pH components and paralleled the rate of appearance of the high pH components. These observations led to suggestions that the pH dependence was associated with both sites (e.g., Henzl & Birnbaum, 1988; McNemar & Horrocks, 1990).

However, we now know unequivocally that the pH dependent behavior is restricted to the CD site. Thus, the signal arising at pH 5.0 from the ion bound at the CD site must include intensity from both visible components of the low-pH spectrum. Furthermore, judging from the spectrum remaining near 579.5 nm after deprotonation of serine-55, the EF contribution must likewise include two components. Observing this residual spectrum with a typical parvalbumin is problematic. Since the pK_a for deprotonation of serine 55 is $\approx$8.25, the pH must be raised above 9.5 before the pH dependent alteration of the CD-site signal is complete. This pH value is sufficiently high that complications arising from lanthanide ion hydrolysis or pH-induced conformational changes in the protein could potentially interfere with the analysis. In the case of oncomodulin, however, the pK_a for deprotonation of serine-55 is only 6.0. As a consequence, the spectral alteration is complete at much lower pH values, enabling us to observe the contribution of the EF site in the spectrum even at pH 8.0. As noted above, accurate modeling of the region near 579.5 nm in the pH 8.0 spectrum requires inclusion of two features. Thus, we are forced to conclude that the signals arising from the ions bound at both the CD and EF sites have (at least) two components.

In favorable cases, we can estimate the relative contributions of the CD and EF sites to the low-pH spectrum. The behavior observed with the wild-type protein serves as an illustrative example. The total intensity near 579.5 nm at pH 5.0 (13.1×10^4) reflects the summed contributions from both sites. At pH 8.0, the CD signal has been quantitatively converted to the high-pH form, so that the residual signal near 579.5 nm represents the contribution of the EF site (2.1×10^4). As noted above, spectral deconvolution indicates that there are two components associated with the EF spectrum and that the EF components largely coincide with the CD components. The difference in intensity (11.1×10^4) near 579.5 at pH 5.0 and 8.0 represents the contribution of the CD signal to the low-pH spectrum. Thus, for the wild-type protein, the contribution of the CD site to the low-pH spectrum is roughly 5 times larger than the EF contribution. Clearly, this analysis is only feasible for variants that undergo the pH dependent spectral alteration (which eliminates S55D and 55/59) and, moreover, undergo the alteration at just one site (which eliminates D94S and 94/98). Table 3 compares the results of this analysis for those variants that meet these criteria.

The appearance of multiple spectral components for each binding site does not necessarily violate the 1:1 correspondence between the number of peaks and number of distinct species predicted by theory for the $^7F_0 \rightarrow {}^5D_0$ transition. The components could reflect, for example, different hydration states of the ion. In the spectrum of Eu^{3+}-EDTA, for example, the peaks at 579.60 and 580.12 nm are known to arise from species having three and two molecules of bound water, respectively. Alternatively, the peaks could conceivably reflect different conformational states of the protein. Whatever the explanation, it seems likely that the two components of the high-pH spectrum have a similar origin.

With the recognition that the CD signal dominates the spectrum and that it has (at least) two components, it becomes easier to reconcile the spectral changes that accompany the CD$\leftrightarrow$EF interconversions. When we began to analyze the spectroscopic data, we were puzzled by two general observations. The first was that the mutations at the EF site of the wild-type protein caused relatively minor changes in the low-pH spectrum. For example, although the D94S mutation drastically reduces the affinity of the EF site for Ca^{2+} (R.C.H. and M.T.H., manuscript in preparation), the apparent Eu^{3+} luminescence parameters are little changed. Similarly, the G98D mutation increases the affinity of the EF site for Ca^{2+} by more than an order of magnitude. Yet, the apparent peak

maxima in the $^7F_0 \rightarrow {}^5D_0$ spectrum at pH 5.0 are virtually identical to those of the wild-type spectrum. We had anticipated that both mutations would be accompanied by substantial alterations in the peak maximum near 579.5 nm that we had previously attributed to the EF site signal. However, these observations become understandable if, as we are suggesting, the EF contribution to the wild-type spectrum is relatively minor and largely overlaps the CD contribution.

Conversely, we observed that mutations at the CD site have substantially greater impact on the appearance of the spectrum and, significantly, cause alterations in both components of the low-pH spectrum. For example, the S55D mutation shifts both components of the low-pH spectrum approximately 0.15 nm to higher wavelength, causes perceptible changes in line width, and reduces the intensity of the higher wavelength component by roughly one-third. Similarly, introduction of the D59G mutation into the S55D variant leaves the peak maxima (at 579.38 and 579.66 nm) and the apparent line widths unchanged. However, the higher wavelength component is approximately doubled in area. These changes would be difficult to rationalize if the two spectral components actually represented the individual binding sites. Since the mutations fall within the CD loop, it would be necessary to invoke a cooperative interaction to explain alterations in the EF signal. On the other hand, if both peaks are components of the CD site signal, it is reasonable that both would be sensitive to mutations within the CD loop.

Eu^{3+} $^7F_0 \rightarrow {}^5D_0$ Spectra Are Sensitive to Both Local and Long-Range Structural Factors. Inspection of Table 3 reveals that the unaltered EF sites in wild-type oncomodulin, S55T, and D59G, as well as the mutated site in G98D, all display comparable intensities between 2.1 and 2.5 $\times 10^4$. Interestingly, the intensity of the EF-site signal is doubled to 5.0 $\times 10^4$ by incorporating a serine residue in place of aspartate-94 at the $+z$ position. A further substantial increase is observed (to 7.1 $\times 10^4$) with the subsequent replacement of glycine-98 by aspartate. These results illustrate, not unexpectedly, that the spectroscopic properties of the parvalbumin binding sites are sensitive to the identity and arrangement of the ligands in the immediate coordination sphere. Note, however, that the intensity of the quasi-CD site resulting from the combined D94S and G98D mutations (7.1 $\times 10^4$) is just 45% of that of the wild-type CD site.

Although the EF-site signal intensity is substantially increased by importing the CD ligand array, the CD-site signal does not appear to suffer a comparable decrease in intensity with importation of the EF ligand array. In fact, comparison of the CD-site intensities for the wild-type protein (11.0 $\times 10^4$) and that of 55/59/94 (12.1 $\times 10^4$) would suggest that the combined S55D and D59G mutations have had essentially no impact on the low-pH signal intensity. The intensity of the CD site in 55/59/94/98 (a quasi-EF site) is somewhat lower (6.8 $\times 10^4$), but still several times greater than that of the wild-type EF site.

Thus, we find that the same ligand array yields a significantly higher intensity when placed in the "context" of the CD site than when placed in the context of the EF site. The signal from the authentic parvalbumin CD site is approximately 55% more intense than the signal arising from the quasi-CD site created within the EF site by the D94S and G98D mutations. Similarly, the signal from the quasi-EF site created within the CD domain by the S55D and D59G mutations is approximately 3 times more intense than the signal arising from the authentic EF site. These findings imply that the metal ion-binding properties of the CD site are strongly influenced by higher order structural considerations as well as by the immediate coordination environment.

Our observations suggest that the folding of the polypeptide chain makes a substantial contribution to the increased rigidity of the parvalbumin CD site. Whereas the CD site is located almost exactly in the middle of the amino acid sequence, the $-z$ ligand of the EF site (glutamate-101) is just eight (β-parvalbumins) or nine (α-parvalbumins) residues from the C-terminus. It seems likely, therefore, that the EF site would enjoy greater conformational flexibility. Alterations in the volume of the binding loop can probably be accommodated by minor adjustments in the orientation of the flanking F helix. By contrast, it is anticipated that reorientation of the helices flanking the CD site would be less facile, since these adjustments would require compensatory changes in the adjacent regions of the polypeptide chain.

Cooperative Interactions between the Oncomodulin CD and EF Sites. The issue of cooperative binding in the parvalbumins has a history of controversy. *A priori*, it would seem unlikely that the the binding events at the CD and EF sites could be completely independent. In common with other EF hand proteins, the two sites are physically adjacent, and their binding loops actually form a short segment of antiparallel β-sheet (e.g., Strynadka & James, 1989), providing a mechanism for transmission of cooperative interactions. However, the magnitude of the interaction and its potential influence on parvalbumin metal ion-binding properties have been long-standing matters of debate. Undoubtedly, part of this disagreement reflects attempts to compare data gathered with diverse experimental techniques on different parvalbumin isoforms (White, 1988). Evidence has accumulated in recent years to suggest that the Ca^{2+}-binding properties are not uniform across the family. Although both parvalbumin ion-binding sites typically belong to the Ca^{2+}/Mg^{2+} category, several exceptions have been noted: oncomodulin (Hapak *et al.*, 1989; Cox *et al.*, 1990), cod III parvalbumin (Hutnik *et al.*, 1990), and the avian thymic parvalbumin called CPV3 (Hapak *et al.*, 1994).

In oncomodulin, as in other parvalbumin isoforms, the cooperativity issue is likewise controversial. Sykes and coworkers (Golden *et al.*, 1989) studied $Ca^{2+}-Lu^{3+}$ exchange in the wild-type protein and the D59E variant by NMR and stopped-flow optical studies. They interpreted their results in terms of a positively cooperative interaction between the two sites. By contrast, Cox *et al.* (1990) concluded from microcalorimetric analyses that the binding of Ca^{2+} to oncomodulin was noncooperative in nature. We have also examined the Ca^{2+}-binding properties of wild-type oncomodulin by microcalorimetry. However, in contrast to the results of Cox *et al.*, our data suggest that the binding of Ca^{2+} to oncomodulin is accompanied by a significant interaction between the CD and EF sites (Hapak & Henzl, 1994). Although the data presented here do not directly address the issue of Ca^{2+} binding, the changes in signal intensity that result from certain of the mutations support claims for cooperativity in oncomodulin. For example, introduction of the G98D mutation into the 55/59/94 variant decreases the intensity of the CD-site signal from 12.1 $\times$ 10^4 to 6.8 $\times 10^4$. The pronounced effect of a mutation in

the EF binding loop on the spectroscopic properties of the CD site argues persuasively for a conformational interaction between the two binding domains.

SUMMARY

We have shown that the presence of a serine residue at the $+z$ position of an EF-hand binding pocket may be sufficient to confer pH dependence on the Eu^{3+} $^7F_0 \rightarrow {}^5D_0$ signal for that site. Secondly, quantitative analysis of the variant spectra forces us to the conclusion that the individual components of the low-pH parvalbumin spectrum are not, as previously believed, site-specific signals for the CD and EF binding domains. Instead, they reflect distinct coordination environments of the bound ions, possibly resulting from differential hydration (cf., Eu^{3+}-EDTA) or conformational heterogeneity.

Although the luminescence properties of the CD and EF sites are sensitive to the identities of the ligands in the immediate coordination sphere, it is clear that the character of the two sites is also dictated to a large extent by the folding of the polypeptide chain. We suggest that the flexibility of the EF site may derive from its proximity to the C-terminus of the protein. Finally, as suggested previously by Sykes and co-workers (Golden *et al.*, 1990), our Eu^{3+} luminescence data attest to the existence of conformational interactions, or cooperativity, between the CD and EF sites.

REFERENCES

Albin, M., & Horrocks, W. DeW., Jr. (1985) *Inorg. Chem. 24*, 895−900.

Brewer, L. M., & MacManus, J. P. (1987) *Placenta 8*, 351−363.

Cox, J. A., Milos, M., & MacManus, J. P. (1990) *J. Biol. Chem. 265*, 6633−6637.

Evans, C. H. (1990) *Biochemistry of the Lanthanides*, Plenum Press, New York.

Gillen, M. F., Brewer, L. M., & MacManus, J. P. (1988) *Cancer Lett. 40*, 151−160.

Gillis, J. M. (1985) *Biochim. Biophys. Acta 811*, 97−145.

Golden, L. F., Corson, D. C., Sykes, B. D., Banville, D., & MacManus, J. P. (1989) *J. Biol. Chem. 264*, 20314−20319.

Haner, M., Henzl, M. T., Raissouni, B., & Birnbaum, E. R. (1984) *Anal. Biochem. 138*, 229−234.

Hapak, R. C., & Henzl, M. T. (1994) *J. Biol. Chem.* (in press).

Hapak, R. C., Lammers, P. L., Parmisano, W. A., Birnbaum, E. R., & Henzl, M. T. (1989) *J. Biol. Chem. 264*, 18751−18760.

Hapak, R. C., Zhao, H., Boschi, J. M., & Henzl, M. T. (1994) *J. Biol. Chem. 269*, 5288−5296.

Heizmann, C. W., & Berchtold, M. W. (1987) *Cell Calcium 8*, 1−41.

Henzl, M. T., & Birnbaum, E. R. (1988) *J. Biol. Chem. 263*, 10674−10680.

Henzl, M. T., McCubbin, W. D., Kay, C. M., & Birnbaum, E. R. (1985) *J. Biol. Chem. 260*, 8447−8455.

Henzl, M. T., Hapak, R. C., & Birnbaum, E. R. (1986) *Biochim. Biophys. Acta 872*, 16−23.

Henzl, M. T., Treviño, C. L., Dvorakova, L., & Boschi, J. M. (1992) *FEBS Lett. 314*, 130−134.

Horrocks, W. DeW., Jr., & Collier, W. E. (1981) *J. Am. Chem. Soc. 103*, 2856−2862.

Horrocks, W. DeW., Jr., & Sudnick, D. R. (1981) *Acc. Chem. Res. 14*, 384−392.

Hutnick, C. M. L., MacManus, J. P., & Szabo, A. G. (1990) *Biochemistry 29*, 7318−7328.

Kretsinger, R. H. (1980) *CRC Crit. Rev. Biochem. 8*, 119−174.

Kretsinger, R. H. (1987) *Cold Spring Harbor Symp. Quant. Biol. 52*, 499−510.

Kretsinger, R. H., & Nockolds, C. E. (1973) *J. Biol. Chem. 248*, 3313−3326.

Lyle, S. J., & Rahman, M. (1963) *Talanta 10*, 1177−1182.

MacManus, J. P. (1979) *Cancer Res. 39*, 3000−3005.

MacManus, J. P., & Whitfield, J. F. (1983) *Calcium Cell Funct. 4*, 411−440.

Martin, R. B. (1983) in *Calcium in Biology* (Spiro, T. G., Ed.) pp 235−270, John Wiley and Sons, New York.

McNemar, C. W., & Horrocks, W. DeW., Jr. (1990) *Biochim. Biophys. Acta 1040*, 229−236.

Palmisano, W. A., Treviño, C. L., & Henzl, M. T. (1990) *J. Biol. Chem. 265*, 14450−14456.

Rhee, M.-J., Sudnick, D. R., Arkle, V. A., & Horrocks, W. DeW., Jr. (1981) *Biochemistry 20*, 3328−3334.

Samelson, H., Brecher, C., & Lempicki, A. (1966) *J. Mol. Spectrosc. 19*, 349−371.

Sowadski, J., Cornick, G., & Kretsinger, R. H. (1978) *J. Mol. Biol. 124*, 123−132.

Strynadka, N. C. J., & James, M. N. G. (1989) *Annu. Rev. Biochem. 58*, 951−998.

Treviño, C. L., Palmisano, W. A., Birnbaum, E. R., & Henzl, M. T. (1991a) *J. Biol. Chem. 265*, 9694−9700.

Treviño, C. L., Boschi, J. M., & Henzl, M. T. (1991b) *J. Biol. Chem. 266*, 11301−11308.

White, H. D. (1988) *Biochemistry 27*, 3357−3365.

Williams, T. C., Corson, D. C., & Sykes, B. D. (1984) *J. Am. Chem. Soc. 106*, 5698−5702.

Williams, T. C., Corson, D. C., Sykes, B. D., & MacManus, J. P. (1987) *J. Biol. Chem. 262*, 6248−6256.

Wnuk, W., Cox, J. A., & Stein, E. A. (1982) *Calcium Cell Funct. 2*, 243−278.

BI9414000